

Optically stimulated luminescence dating of an aeolian dune, occupied during the Final Palaeolithic and Neolithic, along the Upper Scheldt valley at Oudenaarde “Markt” (prov. of East Flanders, BE)

Philippe CROMBÉ, Frédéric CRUZ, Arne DE GRAEVE, Johan DE GRAVE,
Wouter DE MAEYER, Éva HALBRUCKER, Dimitri TEETAERT,
Dimitri VANDENBERGHE & Hans VANDENDRIESSCHE

1. Introduction

Salvage excavations conducted in 2016 by the regional archaeological service SOLVA at the central market of the city of Oudenaarde (NW Belgium) revealed, amidst (post-)Medieval features, remains of an aeolian dune containing prehistoric lithic and ceramic finds. The presence of a silty cap on some of the lithics as well as the deep vertical spread of the artefacts indicated a pre-Holocene age of at least part of the lithic industry. Therefore, it was decided to apply OSL dating in order to determine the chronology of the dune formation in relation to its prehistoric occupation.

2. Site and excavation

The site of Oudenaarde “Markt” is situated on the left bank of the Scheldt River in NW Belgium (coordinates $50^{\circ}50'32.2''/N$ $3^{\circ}36'12.5''E$; Fig. 1), outside the boundaries of the Lateglacial floodplain. Remains of a low-lying SW-NE oriented sandy elevation (ca. 11.50 m TAW = reference height Ostend), were discovered over a length of 143 m and a width of 45 m (Fig. 2). Most of this elevation, however, was disturbed by (post-) Medieval sand extraction pits, leaving only small portions untouched (Fig. 3). Only in two locations, one in the SW and another in the SE, an entire stratigraphic sequence could be recorded (Fig. 4).

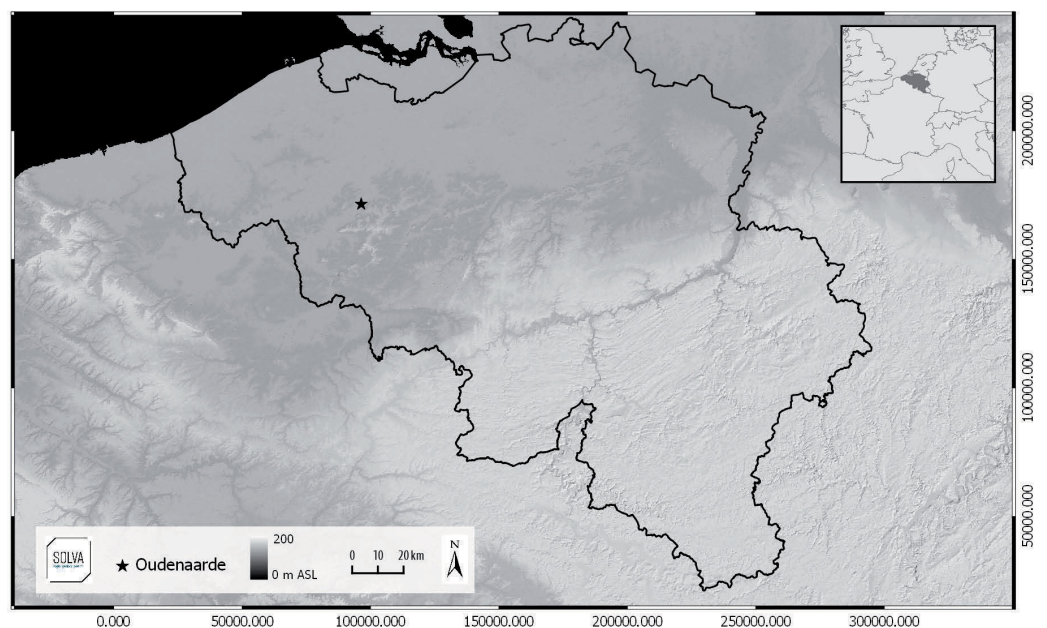


Fig. 1 – Location map of the site of Oudenaarde “Markt” (indicated by the star).



Fig. 2 – Excavation plan showing the extent of the sandy elevation and the parts which have been preserved.



Fig. 3 – Photo of some (post-)Medieval sand extraction pits, which destroyed large parts of the sandy elevation and prehistoric site.

The first prehistoric finds were collected from Medieval extraction pits but it was also noted that some artefacts were present outside features in the undisturbed sandy sediment. At one location in the SW a small concentration of lithic artefacts was observed within the sand. It was decided to excavate this small section over a surface of ca. 11.60 m², partially by means of 1/4 m² squares (Fig. 5) and partially by shoveling the soil into big bags. The latter method was chosen because of the strict timeframe imposed by the planned infrastructural works. The 1/4 m² squares were excavated in artificial layers of 10 cm. Almost all artefacts > 1 cm were registered three-dimensionally and the excavated soil was afterwards wet-sieved through 2 mm meshes.

3. Stratigraphy

Based on the field observations three main stratigraphic units (Fig. 6) can be defined.

Laminated sand: situated at the base of the sequence (layer IV-667). The upper limit of this unit is generally sharp and horizontal. It is composed of greenish sands of fine to coarse texture spotted with concretions of iron-manganese. The greenish color results from the presence of glauconite, possibly indicating reworking of tertiary sediments. These sands are interstratified with more loamy and clayey layers varying from a few centimeters to a few decimeters thickness. This unit most likely consists of alluvial sediments deposited by a braided river system. Locally, a very weakly developed brownish horizon was observed in the top, which might correspond to a paleosol. A quick palynological screening, however, showed that no pollen were preserved in this horizon (analysis A. Storme).

Homogeneous fine sand: deposited immediately on top of the laminated sand (layers IV-666 and IV-775) with a maximum preserved thickness of ca. 1 m. This unit consists of beige fine-grained and well-sorted sands with locally some patches of greenish sands and flint gravel at its base. The upper part of this unit (top 30 to 40 cm; layer IV-775) has a brownish color, possibly resulting from soil formation processes (B-horizon?). This unit can most likely be interpreted as an aeolian deposit forming a dune on top of the floodplain sediments.

Mixed layer: all layers on top of the aeolian sands (IV-192, IV-196, IV-187, IV-190 and IV-743) are anthropogenic in origin and are related to the (post-)Medieval occupation of the site.



Fig. 4 – One of the best-preserved profiles, showing the thickness of the sandy sediments deposited on top of the laminated sands.

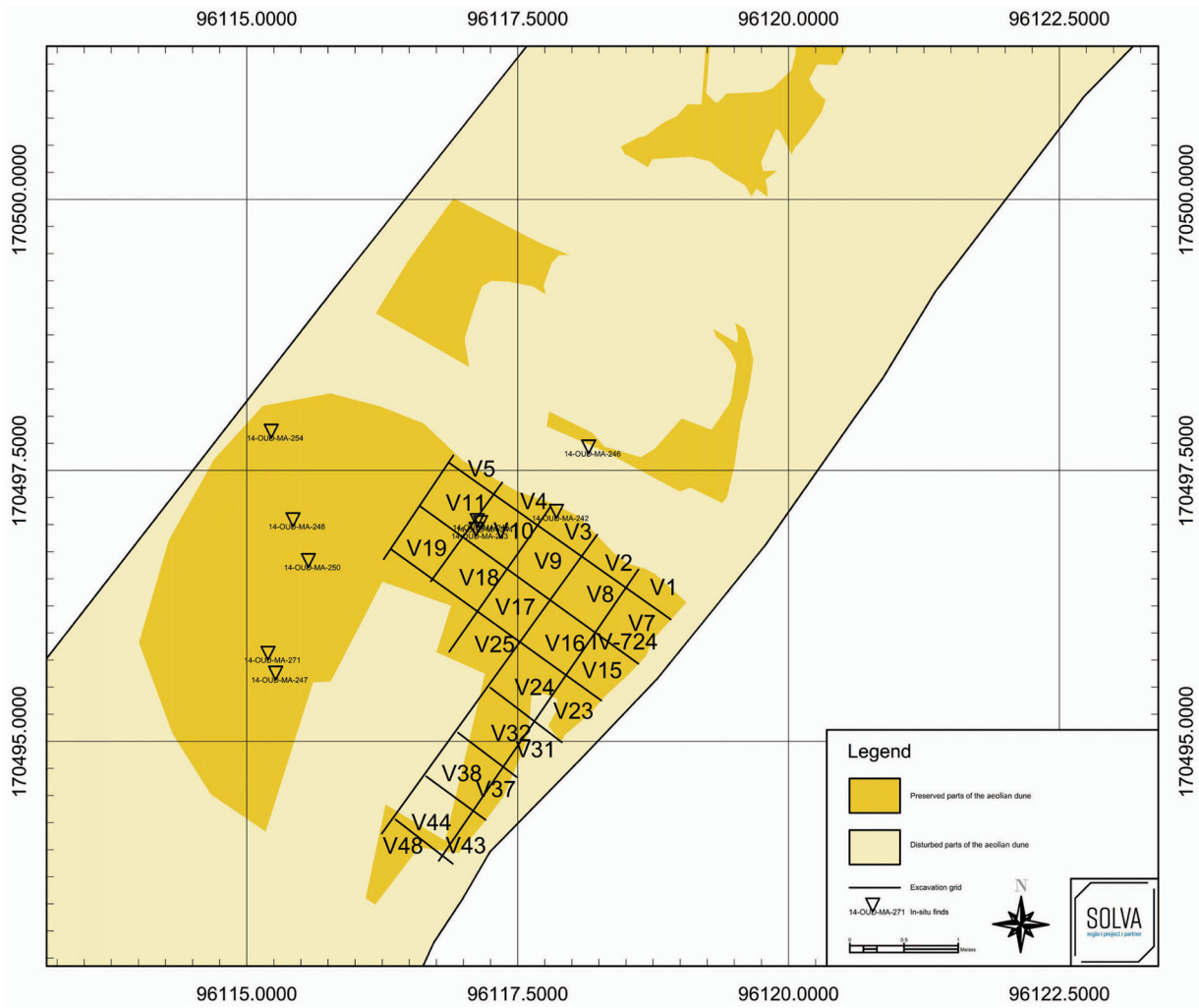


Fig. 5 – Detailed map of the excavated prehistoric site.

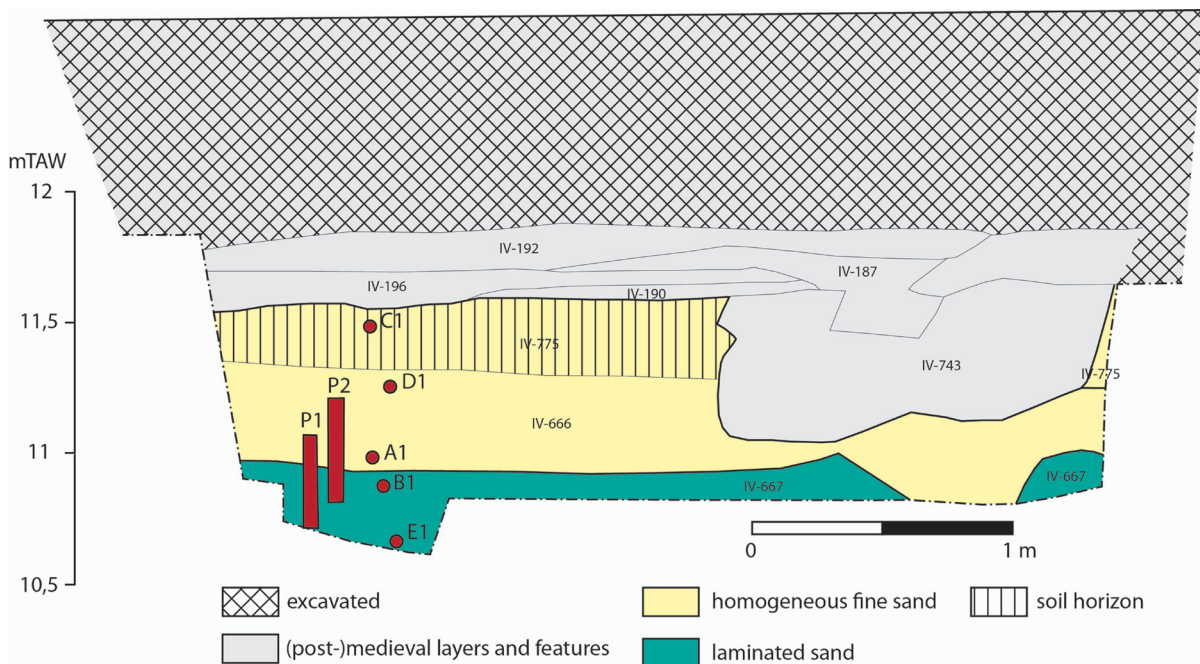


Fig. 6 – Stratigraphical section nearby the prehistoric site with indication of the OSL (A1-E1) and pollen samples (P1-P2).

4. Optically stimulated luminescence (OSL) dating

4.1. Material and methods

Samples for OSL dating were collected by gently hammering opaque PVC tubes into a freshly cleaned exposure. The samples were taken in duplicate; only one of each set (field-codes A1 to E1) was further processed. For each set, about 0.6-0.8 kg of surrounding sediment was collected for dose rate determination. The location of the samples is indicated in figure 6.

In the laboratory, sand-sized (125-180 μm) quartz grains were extracted from the inner material of the sampling tubes using conventional sample preparation procedures (HCl, H_2O_2 , sieving, and HF). The purity of the quartz extracts was confirmed by the absence of a significant infrared stimulated luminescence (IRSL) response at 60°C to a regenerative β -dose. The sensitivity to infrared stimulation was considered to be significant if the OSL IR depletion ratio deviated by more than 10 % from unity (Duller, 2003).

All analyses were carried out on grains spread on the inner 8 mm of 9.7 mm stainless steel discs. The luminescence measurements were made with automated Risø TL/OSL readers, equipped with high power blue diodes emitting at 470 ± 30 nm. Stimulation with infrared light was through IR LEDs (870 or 875 nm). All luminescence emissions were detected through a 7.5 mm thick Hoya U-340 UV filter. Irradiations were carried out with $^{90}\text{Sr}/^{90}\text{Y}$ β -sources mounted on the readers. Details on the measurement apparatus can be found in Bøtter-Jensen *et al.* (2003) and Lapp *et al.* (2015).

The equivalent dose (D_e) was determined using the single-aliquot regenerative-dose (SAR) protocol as described by Murray and Wintle (2000, 2003). Optical stimulation with the diodes was for 40 s at 125°C. The initial 0.32 s of the decay curve, minus a background evaluated from the 0.32-1.12 s interval, was used in the calculations. Preheating of regenerative doses was for 10 s, while the response to the test dose was measured following a cut heat. After measuring the test dose signal, a high-temperature cleanout was performed by stimulating with the blue diodes for 40 s at 280°C (Murray & Wintle, 2003).

For each sample, the dependence of D_e on preheat temperatures in the range of 160-300°C was investigated; the D_e was calculated from the flat ("plateau") region. In addition, a dose recovery test was used (Murray & Wintle, 2003) to test the performance of the SAR laboratory measurement procedure. In this test, aliquots were bleached at room temperature using the blue diodes (2 times 250 s, with a 10 ks pause in between) and given a dose approximating the expected natural dose; they were then measured using the SAR protocol with a preheat of 10 s at 240°C, and a cut heat to either 160°C or 220°C.

Determination of the dose rate was based on high-resolution gamma-ray spectrometry. The sediment from the surroundings of the OSL-tubes was dried (at 110°C until constant weight), pulverised and homogenised. A subsample of ~140-150 g was then cast in wax (e. g. De Corte *et al.*, 2006) and stored for one month before being measured on top of the detector.

The annual dose was calculated from the present-day radionuclide activities using the conversion factors of Adamiec and Aitken (1998). The external beta dose-rate was corrected for the effect of attenuation and etching using the data tabulated by Mejdahl (1979). An internal dose rate of 0.013 Gy ka^{-1} was assumed (Vandenbergh *et al.*, 2008). Both the beta and gamma contributions were corrected for the effect of moisture as

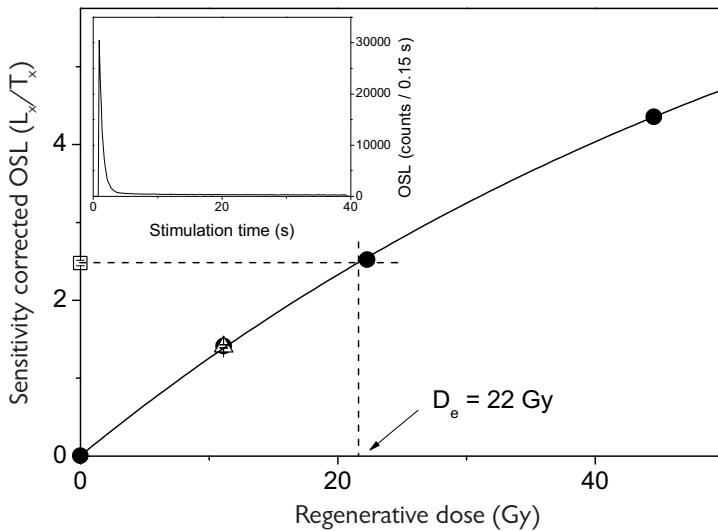


Fig. 7 – Sensitivity-corrected dose-response and natural luminescence decay curve (inset) for an aliquot of quartz grains extracted from sample GLL-163918. The solid line is the fit of the regenerated data (solid circles) to a single saturating exponential function. The equivalent dose (D_e) is obtained by interpolation of the sensitivity-corrected natural OSL signal (open square) on this dose-response curve. The open triangle represents a repeat measurement of the response to a regenerative dose of ~11 Gy (recycling point).

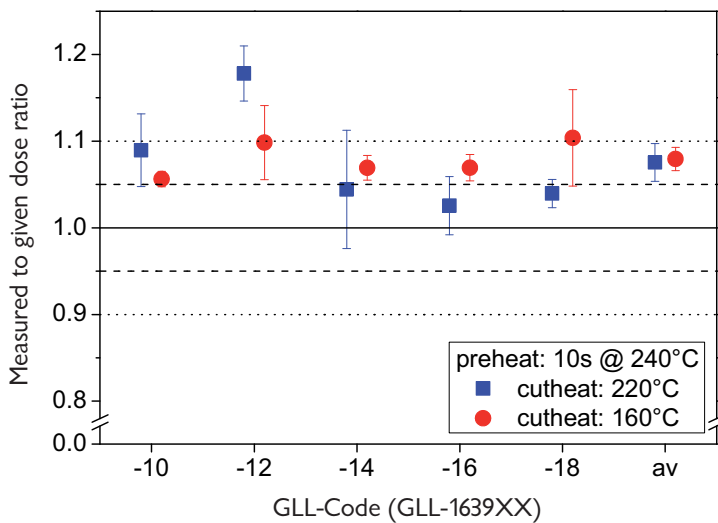


Fig. 8 – Summary of dose recovery data. Red circles and blue squares refer to ratios obtained using a cut heat to 160°C and 220°C, respectively; in both sets of experiments, a preheat of 10 s to 240°C was used. The solid line (eye guide) represents an ideal measured to given dose ratio of unity; the dashed and dotted lines (eye guides) bracket a 5 % and 10 % deviation from unity, respectively.

outlined by Aitken (1985). The contribution of cosmic radiation was calculated following Prescott and Hutton (1994).

The luminescence age for a sample was calculated by dividing the D_e by the effective dose rate. Ages are expressed in ka (1000 a) calendar years before 2016 AD. Uncertainties on the luminescence ages were calculated following the error assessment system proposed by Aitken and Allred (1972) and Aitken (1976). All sources of systematic uncertainty were as quantified by Vandenberghe et al. (2004; see also Vandenberghe, 2004).

4.2. Results

Figure 7 shows a representative dose-response and OSL decay (inset) curve for an aliquot of sample GLL-163918. As commonly observed for this type of material, the luminescence signal decays rapidly with stimulation time; this is characteristic for a quartz-OSL signal that is dominated by the fast component. The dose-response curve could be well approximated by a single or a double saturating exponential function. The recycling point (open triangle in Fig. 7) matches the result of a prior measurement of this dose point, and the growth curve passes through the origin. This indicates the generally good behaviour of the samples in the SAR protocol; sensitivity changes occurring throughout a SAR measurement sequence are accurately corrected for, and thermal transfer of charge from one measurement cycle to the next is negligible.

The results from the dose recovery test are summarised in figure 8. Using the standard set of measurement parameters (involving a preheat of 10 s at 240°C and a cut heat to 160°C), an overall average measured to given dose ratio (± 1 standard error) of 1.08 ± 0.01 ($n = 15$; red circles in Fig. 8) was obtained. Increasing the cut heat to 220°C did not improve the ability to

measure a known laboratory dose administered to a completely-reset sample prior to any heat treatment (blue squares in Fig. 8; overall dose recovery: 1.08 ± 0.02). In both sets of experiments, recycling ratios were consistent with unity (0.99 ± 0.01) and recuperation remained below 0.1 % of the corrected natural OSL signal.

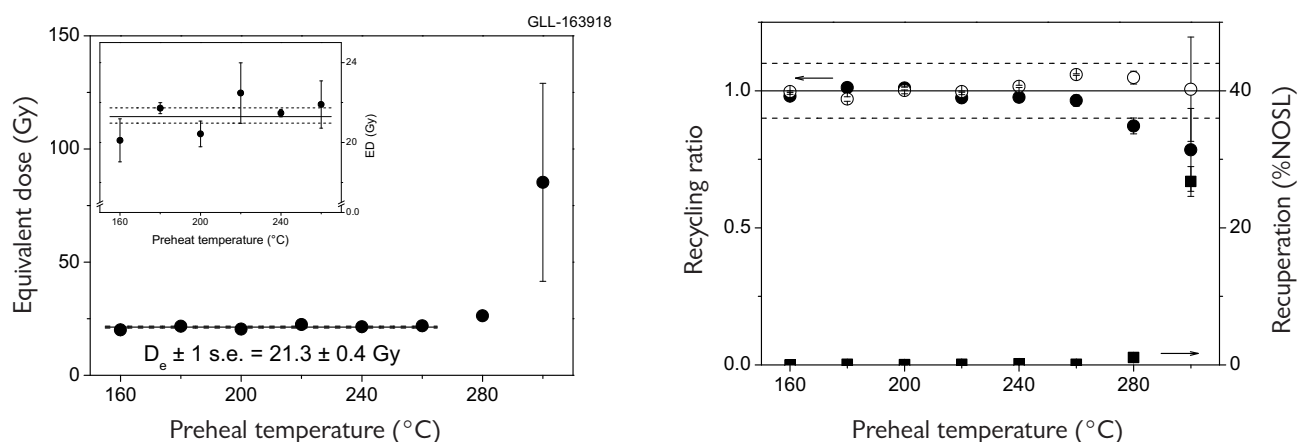


Fig. 9 – Dependence of equivalent dose (D_e) on preheat temperature (left). Each data point represents the average (± 1 standard error) of three measurements. The unweighted average (± 1 standard error) over the 160°C – 260°C preheat temperature range is indicated by the solid and dashed lines. The corresponding recycling and recuperation data are shown in the right graph. The solid and dashed lines bracket a recycling ratio of 1.0 ± 0.1 .

The samples showed no systematic dependence of D_e on preheat temperatures ranging from 160°C to 260°C. This is illustrated in figure 9, using the results obtained for sample GLL-163918. Across this plateau region, recycling ratios are within the range of acceptability (from 0.90 to 1.10) as suggested by Murray and Wintle (2000), while recuperation remains below 0.1 % of the corrected natural OSL signal.

Table 1 summarises the results relevant to the age and uncertainty calculation. If it is assumed that sources of systematic uncertainty are largely shared between the samples, only the sources of random uncertainty can be considered to evaluate the internal consistency of the OSL ages. The optical ages for the four uppermost samples range between 5.8 ± 0.5 ka and 16.8 ± 0.5 ka, and are consistent with the stratigraphic position of the samples. The date of 13.2 ± 0.3 ka for the lowermost sample (GLL-163918) does not fit in this sequence. This apparent age inversion is not understood at present.

For non-windblown deposits, the possibility exists that the OSL clock was incompletely reset. Incomplete resetting leads to age overestimation. Similarly, post-depositional

GLL-code	Field code (depth)	^{40}K (Bq kg^{-1})	^{234}Th (Bq kg^{-1})	^{226}Ra (Bq kg^{-1})	^{210}Pb (Bq kg^{-1})	^{232}Th (Bq kg^{-1})	w.c. (%)	Total dose rate (Gy ka^{-1})	D_e (Gy)	Age (ka)	σ_r (ka)
GLL-163914	C1 (110 cm)	234 ± 3	16 ± 2	17.9 ± 0.4	17 ± 1	15.6 ± 0.2	12 ± 3	1.35 ± 0.02	7.8 ± 0.7	5.8 ± 0.7	0.5
GLL-163916	D1 (140 cm)	241 ± 2	16 ± 2	16.2 ± 0.5	18 ± 1	14.9 ± 0.2	12 ± 3	1.37 ± 0.02	16.1 ± 0.3	11.8 ± 1.1	0.3
GLL-163910	A1 (160 cm)	250 ± 4	13 ± 1	16.4 ± 0.7	15 ± 2	14.5 ± 0.2	19 ± 5	1.25 ± 0.03	21.0 ± 0.4	16.8 ± 1.5	0.5
GLL-163912	B1 (170 cm)	307 ± 3	14 ± 1	21.8 ± 0.4	19 ± 2	18.8 ± 0.3	22 ± 2	1.47 ± 0.02	24.5 ± 0.6	16.6 ± 1.1	0.5
GLL-163918	E1 (190 cm)	347 ± 3	14 ± 1	21.7 ± 0.8	21 ± 1	21.0 ± 0.3	22 ± 2	1.62 ± 0.02	21.3 ± 0.4	13.2 ± 0.9	0.3

Tab. 1 – Radionuclide activities, estimates of past water content (w.c.), calculated dose rates, D_e values, optical ages and random uncertainties associated with the ages. The uncertainties mentioned with the age results are the total uncertainties (i. e. including the contributions from sources of systematic uncertainty); all uncertainties represent 1σ .

disturbances (such as bioturbation) may lead to erroneous depositional ages. Methods to detect and/or allow for these issues have been developed (e. g. Wallinga, 2002; Vandenberghe et al., 2009) but are not part of a standard OSL-dating routine (or at least not for samples in the age range under consideration here). Another factor that may affect the accuracy or observed scatter in age results, are variations of the dose rate with time (Murray & Olley, 2002). In most cases however, one can only assume that the present-day dose rate prevailed throughout the entire period of burial.

5. Prehistoric finds

5.1. Lithic artefacts

5.1.1. Artefacts from the dune sediments

5.1.1.1. Raw material analysis

In terms of the raw material exploitation (Fig. 10), the artefacts recovered from the sandy sediments constitute a remarkably homogeneous assemblage. Ca. 91 % (of the artefacts > 1 cm) are made of a fine-grained flint, displaying a dark grey and translucent outer rim, right underneath the cortex, that quickly evolves into an opaque, light-grey inner area riddled with inclusions. The cortex of this flint type is generally thin and only slightly rolled, whereas frost fractures appear to be absent. The raw material of the majority of the remaining artefacts could not be specified, due to discoloration by heating and weathering events (patination) and the advanced fragmentation of some of the artefacts.

Compared to other recently excavated prehistoric sites from the Upper-Scheldt basin, e. g. Oudenaarde-Donk (Lombaert et al., 2007), Ruien-Rosalinde (Crombé et al., 2014) and Kerkhove-Stuw (Sergant et al., 2016), the so-called Scheldt flint (Vandendriessche et al., 2015: 16) seems, with only one example, underrepresented in this assemblage.

Ca. 2 % (n = 41 artefacts) present traces of burning, among which 24 overheated artefacts. A silty cap occurs on at least 8 larger artefacts; it is reasonable to assume that it was originally present on much more artefacts but was removed during the water sieving (see 2).

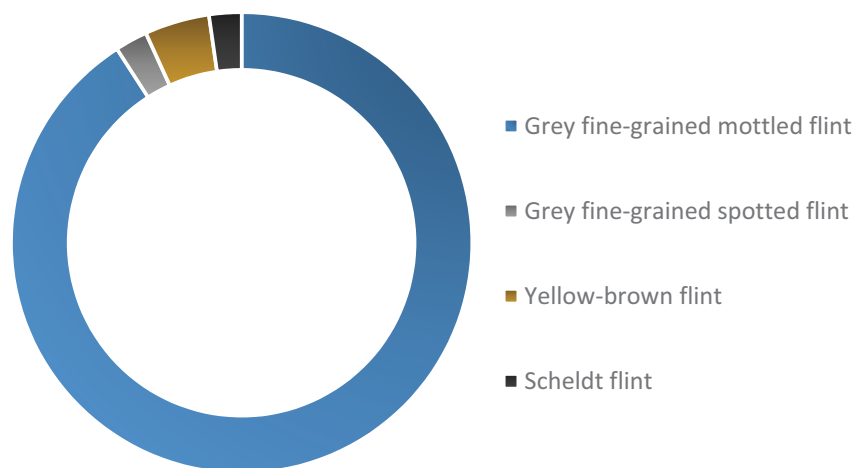


Fig. 10 – Raw material spectrum of the lithic assemblage from the sandy dune sediments.

5.1.1.2. Technological analysis

As demonstrated by the scraper and the multiple burin (see 5.1.1.3), the formal tool types within this assemblage are seemingly derived from reduction sequences aimed at the production of long (> 6 cm) and regular blades (Tab. 2). Besides these, knapping sequences were equally invested in producing numerous short and narrow bladelets, most of which present a straight profile and a linear or punctiform striking platform, in case the proximal part was preserved (n = 15).

Although the dorsal scar pattern of the bladelets indicates a prevalent unidirectional reduction, other data concerning the specific knapping methods employed is scarce. Noteworthy in this regard is a unilaterally crested blade of *néo-crête* type (Fig. 13:2) informing us of a rejuvenation phase occurring during the knapping, most likely to readjust the longitudinal convexity of the flaking surface. Besides that, a core (Fig. 13:4) retrieved from a secondary context, but tentatively belonging to the same lithic assemblage on the basis of the presence of a silty cap, offers us some additional information. It has an almost pyramidal shape and displays the final stages of a bladelet reduction, organised from two opposing, faceted striking platforms and covering 3/4th of the circumference of the core. Finally, the remains of what seems to have been a posterior crest are situated at the back of the core.

Even though the technological data deriving from this assemblage is fragmentary at best, the dual objectives of the knapping sequences and the investment in core shaping and rejuvenation using frontal and posterior crests seemingly evokes Final Palaeolithic technological traditions (e. g. Valentin, 1995; Bodu, 2000; Johansen & Stapert, 2000; Naudinot, 2013; Berg-Hansen, in press).

5.1.1.3. Toolkit

Only three retouched artefacts and one artefact with possible use retouches (ca. 2 %) were collected from the dune sand deposit (Tab. 3). One of these is a multiple burin on a blade (Fig. 13:1), presenting spall negatives on 3 edges. Both the proximal and the distal end were directly truncated in order to create a platform for the burin blows. A second tool may be classified as a scraper on a blade (Fig. 11:2); the scraper front, situated at the proximal blade end, is partially destroyed by a burin-like removal. The latter may be accidentally produced during the use of the left edge of the blade for whittling plant material (see 5.1.1.4). A last retouched tool (Fig. 12:2) is a flake presenting irregular discontinuous retouch along its left edge. All four tools were covered on their ventral side by a silty cap. The latter was also preserved on a scraper found in a secondary context (cf. 5.1.2.2).

5.1.1.4. Use-wear analysis

Although hampered by the small size and fragmentation of the artefacts, as well as by the frequent heating damage, an exploratory microwear analysis was performed on the assemblage from the sand dune deposits. A total of ten artefacts from this context and one additional artefact from a secondary context

	<i>in situ</i>	%	secondary contexts	%
Chip	125	67.57	14	10.69
Bladelet (fragment)	4	2.16	7	5.34
Blade (fragment)	1	0.54	3	2.29
Flake (fragment)	30	16.22	55	41.98
Debris	6	3.24	11	8.40
Undetermined fragment	11	5.95	10	7.63
Potlid	1	0.54	-	-
Core	-	-	3	2.29
Rejuvenation artefact	1	0.54	2	1.53
Burin spall	1	0.54	-	-
Retouched tool	4	2.16	26	19.85
Chip with retouch	1	0.54	-	-
<i>Total</i>	<i>185</i>	<i>100.00</i>	<i>131</i>	<i>100.00</i>

Tab. 2 – Typological inventory of the lithic assemblages collected from the dune sands (*in situ*) and secondary contexts.

	<i>in situ</i>	secondary contexts
Scraper	1	5
Burin	1	-
Strike-a-light	-	3
Retouched flake	1	1
Notched flake	-	1
Bifacially retouched flake	-	1
Retouched blade(let)	-	2
Pointed blade	-	1
Armature	-	3
Artefact with use retouch	1	4
Polished fragment/flake	-	3
Undetermined tool fragment	-	2
<i>Total</i>	<i>4</i>	<i>26</i>

Tab. 3 – Typological inventory of the lithic tools collected from the dune sands (*in situ*) and secondary contexts.

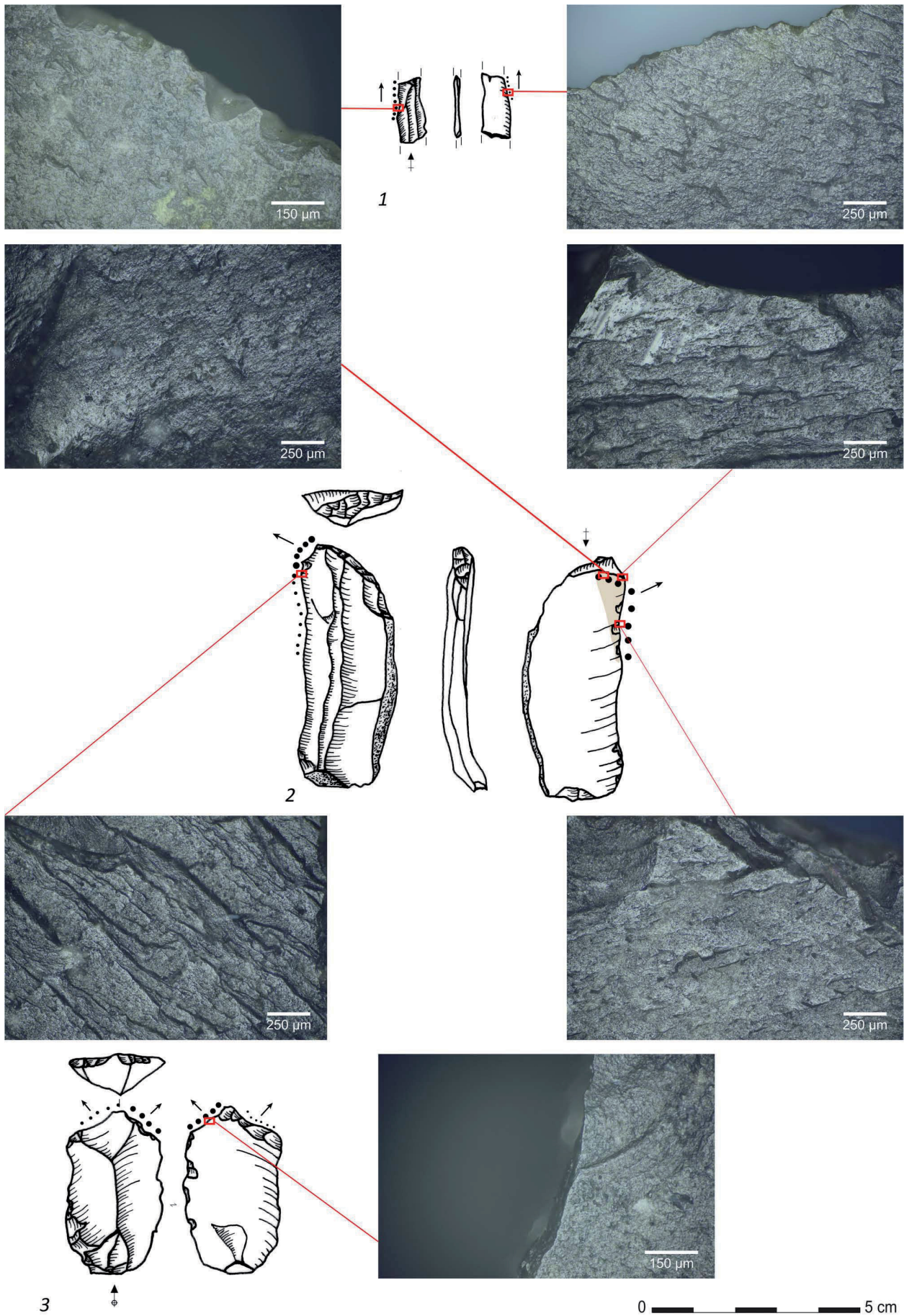


Fig. 11 – Lithic artefacts from the sandy dune sediments, with indication of their use-wear traces.

were subjected to a careful examination using low and high power approach (van Gijn, 1990; 2014).

Some artefacts were heavily covered with sediment that was partly cemented on their surface (i. e. silty cap). Therefore, a precise cleaning protocol was used with the following steps:

1. careful washing by hand with warm water and washing soap;
2. placing the artefacts in ultrasound cleaner with distilled water and Derquim phosphate free soap for 30 minutes;
3. careful washing with warm water by hand;
4. air drying.

After the cleaning, all 11 pieces were looked at with an Olympus SX7 stereo microscope at 40 x magnification. Seven of these were selected for further analysis under higher magnification (100 x and 200 x) using an Olympus BX53 reflected light microscope.

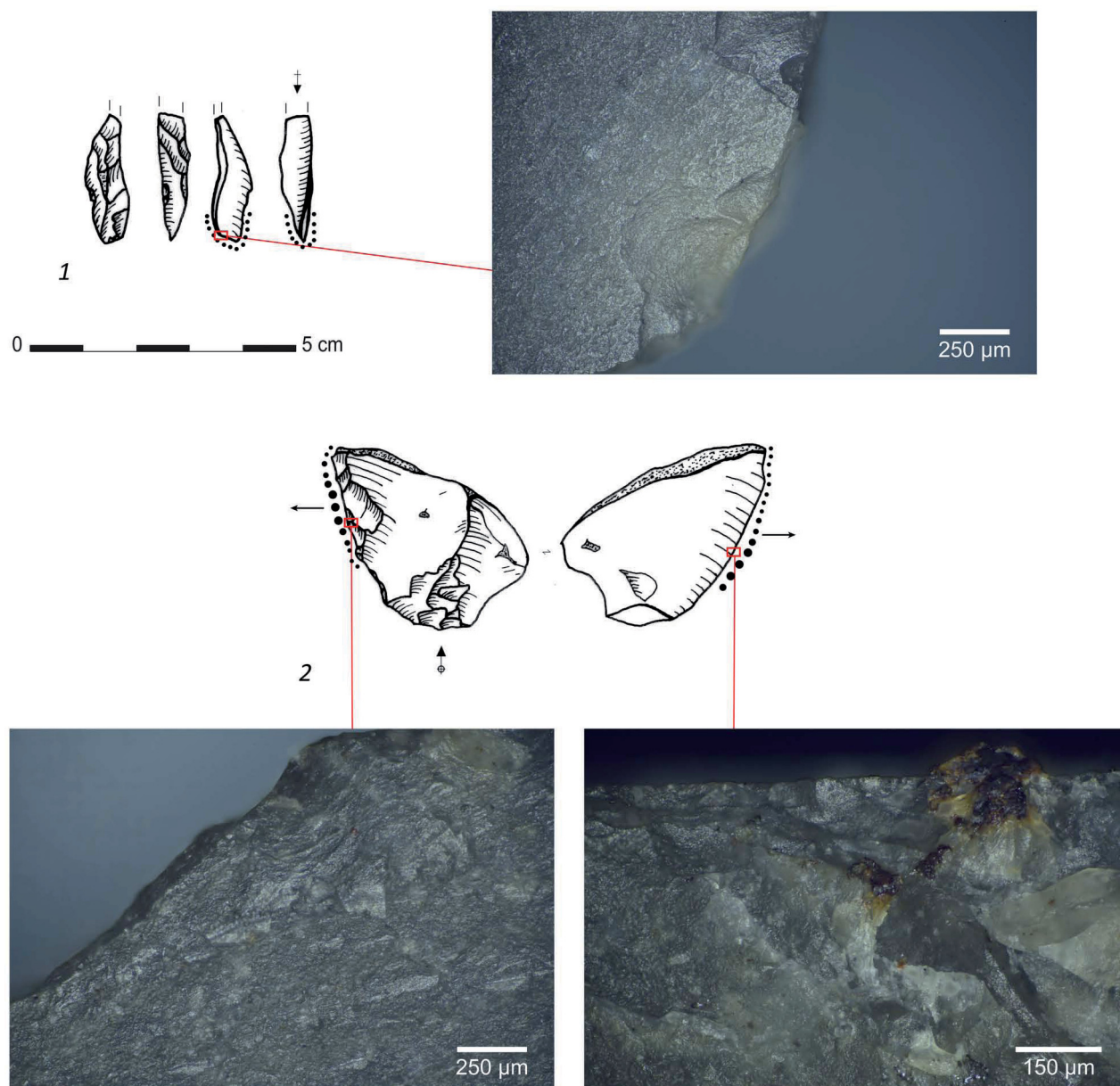


Fig. 12 – Lithic artefacts from the sandy dune sediments, with indication of their use-wear traces.

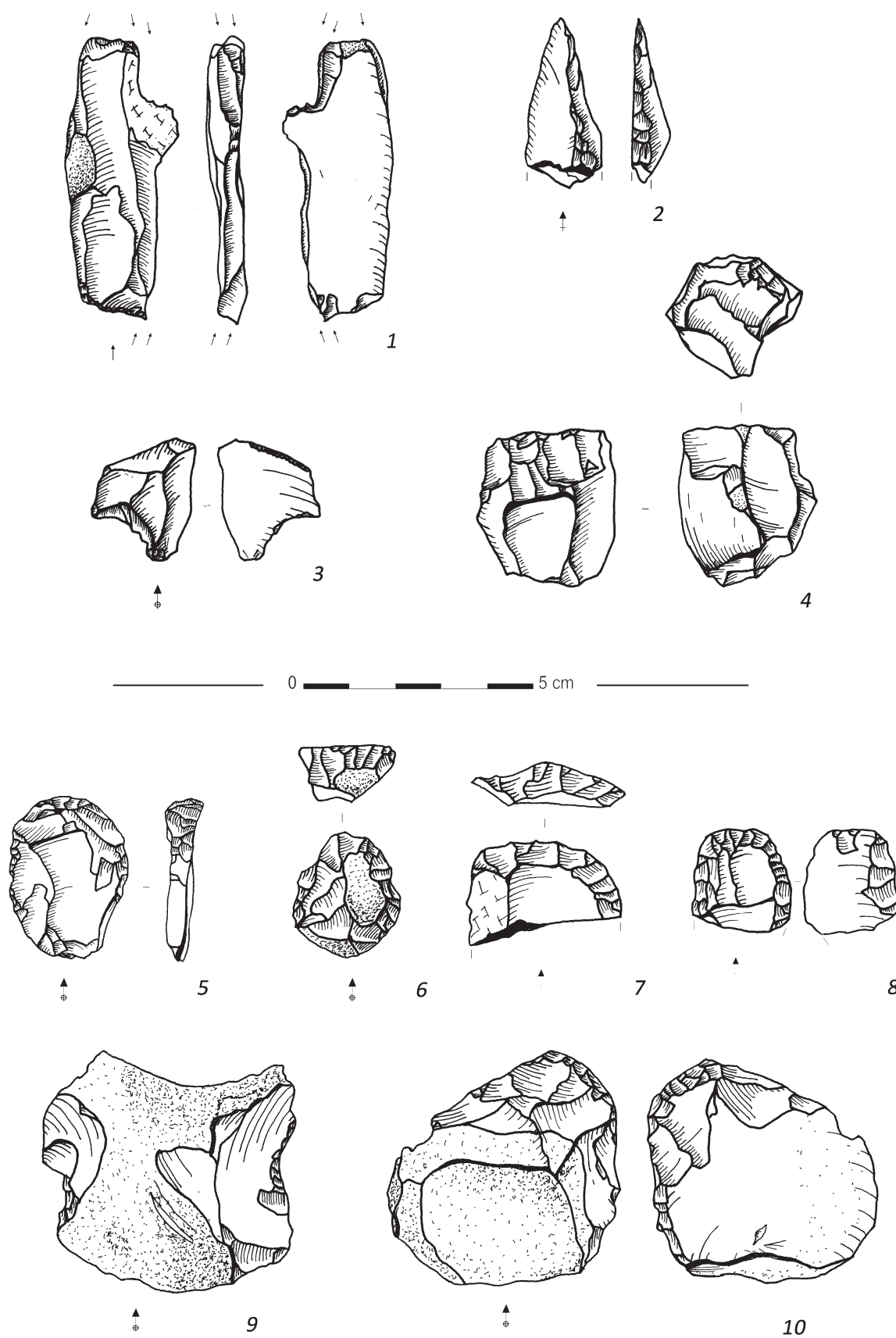


Fig. 13 – Lithic artefacts from the sandy dune sediments (top) and the (post-)Medieval extraction pits (bottom).

Five artefacts yielded interpretable microtraces of use, of which two displayed traces of working plant material (Tab. 4). One small medial bladelet fragment showed traces of cutting semi-hard plant material, probably woody plant (Fig. 11:1). A piece that was typologically categorized as a scraper on blade presented well-developed traces of whittling Si-rich or woody plants, interestingly not on the scraper front, but on the straight edge and the ventral surface (Fig. 11:2). Another scraper yielded traces of scraping dry skin. It also shows microcracking and some gloss caused by slight burning (Fig. 11:3). A burin spall shows developed traces of engraving bone or antler (Fig. 12:1). Last but not least, a retouched flake displays traces of scraping semi-hard material with mineral content that might have been some type of adhesive; apart from these traces, the used edge exhibits an orange residue overlain with the micropolish and an additional black residue occurs on the dorsal surface, somewhat below the used part of the retouched edge (Fig. 12:2).

Despite its limited size, we can conclude that the studied assemblage yielded traces of a wide range of contact materials and activities.

type	polish	development	striations	directionality	distribution	edge damage	contact material	motion
retouched flake (Fig. 12-2)	smooth, flat, matt, very bright, pitted, more on higher parts	developed	thin, short, shallow	transversal	thin line along the edge, ventral side spread in the background	lots of small, irregular scars, in multiple layers	semi-hard material with mineral content	scraping
scraper on blade (Fig. 11-2)	smooth, domed, matt, bright, pitted more on higher parts	well developed	thin, long shallow	transversal	along the edge	few large scars, rounded edge	Si-rich/woody plant	whittling
burin spall (Fig. 12-1)	smooth, flat, matt, bright	developed	no	mixed	thin line along the edge, only ventral side	minimal small scars, rounding	bone/antler	engraving
medial bladelet fragment (Fig. 11-1)	smooth, flat, matt, bright, pitted	developed	no	transversal	spread in the background	small scars during use	semi-hard material	cutting
scraper (Fig. 11-3)	rough, flat, matt, bright, pitted	developed	thin, short, shallow	transversal	along the edge	rounded	dry skin	scraping

Tab. 4 – Description of the use-wear traces observed on five lithic artefacts.

5.1.2. Artefacts from secondary contexts

5.1.2.1. Raw material analysis

A slightly more diverse picture emerges when examining the raw material characteristics of the artefacts retrieved from secondary contexts (Fig. 14). Most of these appear to be made of fine-grained, grey flint varieties ($n = 48$), implying their association (at least in part) to the above described assemblage from the undisturbed dune sediments. This seems corroborated by the discovery of at least two artefacts still presenting a silty cap. A small assemblage ($n = 12$) of Neolithic artefacts (i. e. the pointed blade and polished axe fragments) are produced in high-quality mined flint. Finally, the raw material of a large group of artefacts ($n = 66$) could not be specified for the same reasons as mentioned above, although only ca. 15 % ($n = 19$) of this secondary assemblage presents traces of burning.

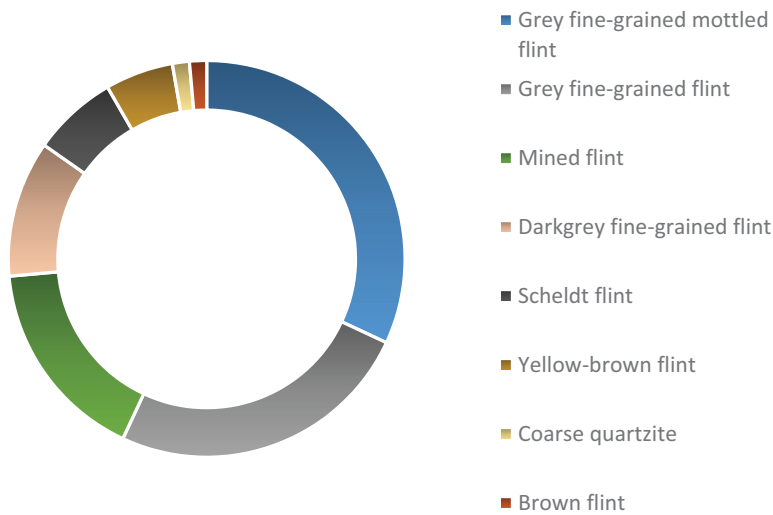


Fig. 14 – Raw material spectrum of the lithic assemblage from the (post-)Medieval extraction pits.

5.1.2.2. Typology

With ca. 20 %, the retouched tools are much better represented compared to the dune assemblage (Tab. 3). This, however, is clearly due to the different excavation method (shovelling versus sieving). Scrapers (5 ex.; Fig. 13:5-8), simply retouched artefacts (5 ex.) and artefacts with possible use retouches (4 ex.) dominate the assemblage. The presence of a silty cap on the ventral side of one of the scrapers (Fig. 11:3) proves it originally was deposited in the dune sediments, and hence this tool can be linked to the “in situ” assemblage. This scraper, which also revealed clear traces of use (see 5.1.1.4), is rather atypical as the distal scraper front has

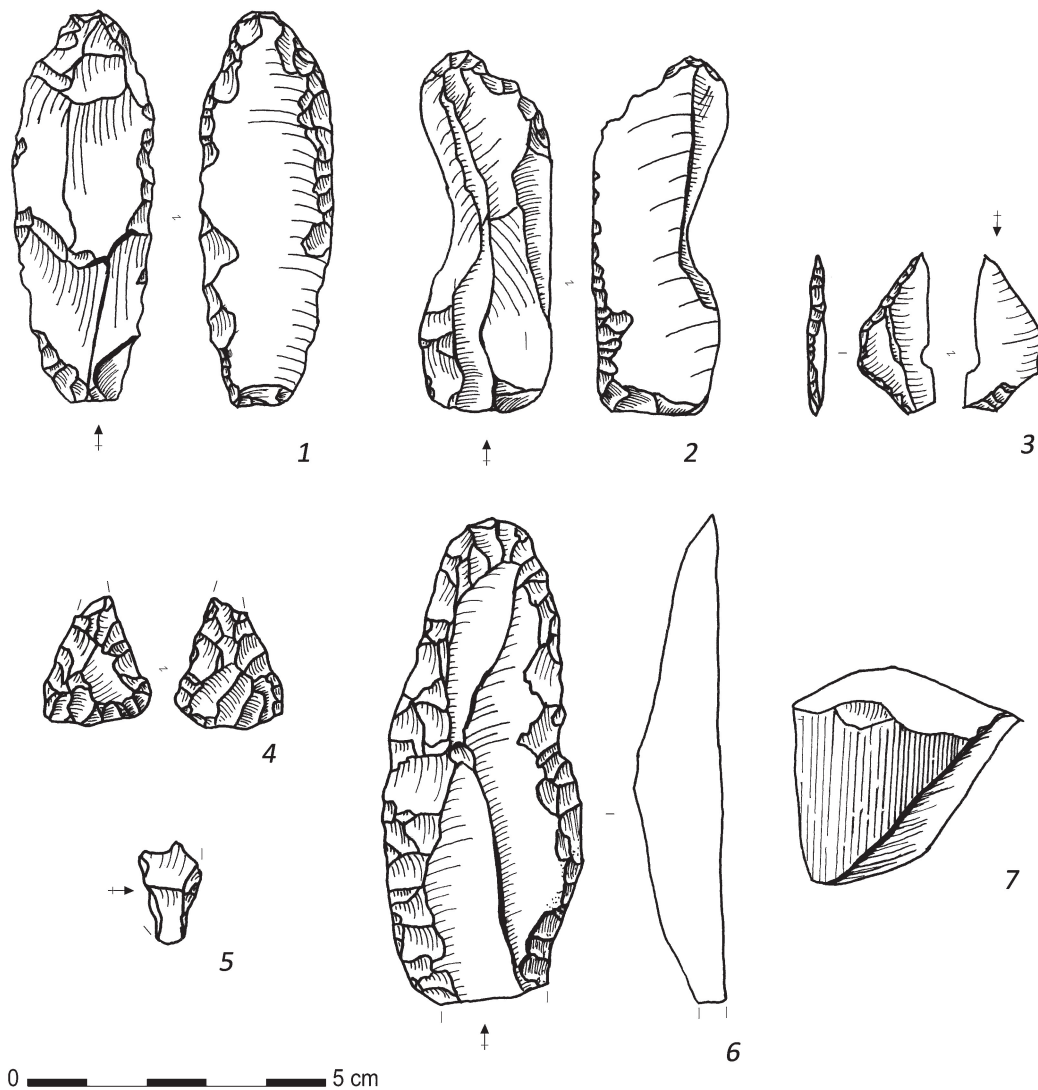


Fig. 15 – Lithic artefacts from the (post-)Medieval extraction pits.

been produced by means of ventral (left side) and dorsal (right side) retouches. Both the left and right edge display irregular and discontinuous retouches. The remaining scrapers consist of two fragments and one intact specimen. Among the latter is a scraper made on the distal end of a large flake (ca. 4 cm), resembling horseshoe-shaped scrapers from the Neolithic (Fig. 13:5). Two out of the three scrapers are smaller (ca. 2 cm) and present an oblique retouch which also covers part of the edges (so-called retouched scrapers; Fig. 13:6, 8). Among the retouched artefacts there are two specimens made on a thick and massive flake: one displays two deep opposite notches (Fig. 13:9), the other one presents bifacial, flat “retouches” along its distal end, which might result from its use as wedge (Fig. 13:10). Among the two fragments of retouched bladelets there is one proximal fragment with a flat ventral retouch. Three artefacts, among which a fragment, can most likely be determined as strike-a-lights based on the presence of a rounded end. Two of these are made on a bladelike blank. A first one on greyish flint (Fig. 15:1) has a rounded distal end; additionally both edges present an almost continuous, but irregular ventral retouch. The second example (Fig. 15:2), made on a thick irregular blade in light brownish, fine-grained flint, displays a similar retouch along its right edge. On the left side two burin-like negatives are visible, which most likely are accidentally produced during its use as strike-a-light. Among the armatures there is a microlith which can be classified as an atypical “evolved” trapeze (Fig. 15:3). The proximal truncation is connected to the bifacially retouched basis, though by means of a series of small irregular and oblique retouches. A small triangular arrowhead with slightly convex base (Fig. 15:4), is bifacially retouched by means of a flat and invasive retouch. Finally there is a small blade fragment in high-quality, light-greyish and fine-grained flint presenting at the distal end a clear truncation (Fig. 15:5). Although the opposite end is broken, it can be assumed that this is a fragment of a transverse arrowhead. Interesting is also the presence of an almost intact pointed blade (Fig. 15:6) made on a dark greyish medium-grained flint, covered by a dull greyish patina. This tool is made on a broad and rather thick blade; both edges are intensively retouched by an oblique and long retouch in a continuous way, forming a pointed end at the distal side. Finally we mention the presence of three artefacts with clear traces of polishing, among which one axe fragment in light-greyish mined flint (Fig. 15:7) and two polished flakes.

5.1.3. Interpretation

Based on the raw material composition, it seems that the lithic artefacts from the dune sediments form a rather homogeneous assemblage, meaning that they most likely belong to the same occupation “event” of the site. Unfortunately, the limited size of this assemblage hampers a chronological interpretation. Except for the burin, which displays clear Final Palaeolithic affinities, no diagnostic tools are present. This tentative date is further supported by some technological features as well as by the presence of a silty cap on a limited number of artefacts. The latter proves that at least these artefacts have been exposed to repeated freeze-thaw cycles, typical of periglacial contexts (Van Vliet-Lanoë, 1985) and hence points to a pre-Holocene age.

Without any doubt some of the finds from the secondary contexts, among which a scraper and a core with a silty cap, also belong to the Final Palaeolithic. Yet the majority of retouched tools from these disturbed contexts are clearly younger. There are only few indications, among which a trapeze, for a Mesolithic presence on the dune. The Neolithic on the other hand seems much better represented. The polished fragments, the pointed blade, the large scraper and the triangular and transverse arrowheads clearly refer to human activities during one or several phases of the Neolithic. Similar artefacts have been found in the 1980s at the wetland site of Oudenaarde “Donk”, situated just ca. 1 km further south along the same river bank (Parent *et al.*, 1986-1987).

5.2. Pottery

Furthermore, Neolithic ceramic remains consisting of 16 sherds (90 g) and 62 g undetermined small fragments were discovered. Their surfaces are weathered and encrusted with sandy sediment that is difficult to remove. Ten wall fragments (5-11 mm thick) and one small rim fragment with rounded lip are tempered with burnt flint, possibly in combination with grog. N-joints and quadrangular fractures point to the use of the coiling technique. Based on these technological features, this pottery most likely can be dated to the middle Neolithic (Michelsberg Culture/Spiere group) period as known in the Scheldt basin (Vanmontfort, 2001; Bostyn et al., 2011). In the five remaining fragments no visible temper is observed.

5.3. Vertical distribution

Due to the difficult excavation conditions there is little information on the precise stratigraphical position of the archaeological finds within the dune sediments. Clearly the lithic artefacts occurred vertically spread over the entire depth of the sediment (Fig. 16), however with a peak more or less halfway the sediment (11.30-11.20 m TAW), which corresponds with the transition towards the B-horizon. A second smaller “peak” is situated near the base of the dune sediments (11.10-11.00 m TAW). However, it seems that only smaller items, mainly chips, occur at this level. Whether this points to two separate “occupation levels” or artefact migration due to either upfreezing (Johnson et al., 1977; Gozdzik & French, 2004; Kaplar, 1965; Van Vliet-Lanoë, 1985) or bioturbation is difficult to assess due to the limited stratigraphical precision. The former process leads to an upwards displacement of mainly larger artefacts, while the latter results in a downwards migration, which mainly affects the smaller artefacts. So, both mechanisms can result into a size-sorting of the artefacts. In the absence of clear periglacial features, such as frost cracks, upwards migration might be ruled out, although the presence of a silty cap on different larger artefacts clearly indicates repeated freeze-thaw cycles. The vertical spread of the handmade pottery on the other hand clearly is limited to the B-horizon, developed in the top of the dune sediments.

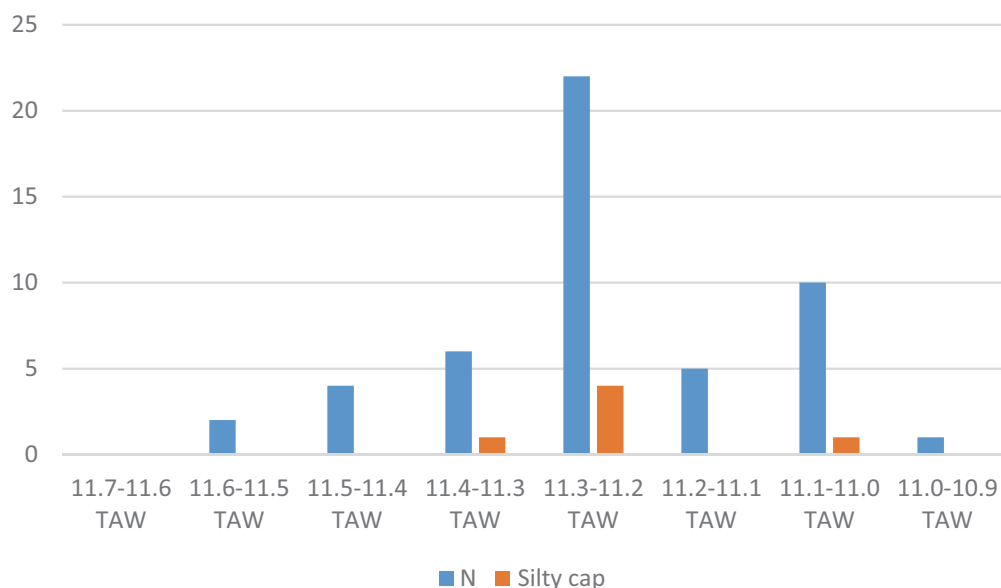


Fig. 16 – Vertical distribution of the lithic artefacts (absolute numbers) and artefacts with silty cap in the dune sediments.

6. Discussion

6.1. Dune formation

The OSL dating program conducted at Oudenaarde demonstrates the importance of collecting multiple samples, at closely-spaced intervals and in a well-defined stratigraphical framework, from a single locality. It provides an internal check of consistency. The inherent ability to detect inconsistencies not only minimises the risk of erroneous interpretation, but also paves the way to methodological improvement. Ideally, the set of duplicate samples was OSL-dated as well; this was not possible within the frame of this work and, admittedly, such a strategy may in general require too much means to be feasible in practice.

Despite this, the OSL results are consistent with the lithostratigraphy except the lowest sample (GLL-163918), which clearly is too young. Sample GLL-163912 (16.6 ± 1.1 ka) confirms the final Pleniglacial age of the laminated sands, interpreted as deposits of a braided river system. The base of the sandy sediments is dated to the same time-range (GLL-163910; 16.8 ± 1.5 ka), indicating that aeolian activity started as early as the final Pleniglacial. The OSL-date for sample GLL-163916 (11.8 ± 1.1 ka), which was collected in the middle of the sand dune sediments, perfectly fits with other dates obtained on similar dunes in alluvial context along the Scheldt River, which demonstrate that most of these were formed mainly during the Younger Dryas (Bogemans & Vandenberghe, 2011). Finally, the uppermost sample GLL-163914 suggests that wind deflation continued or more likely was reactivated during the mid-Holocene. However, given its stratigraphical position in the soil horizon relatively close to the dune top, it cannot be excluded that this date is erroneous due to post-depositional processes, such as bioturbation and soil formation.

6.2. Prehistoric occupation

The archaeological finds, including lithic artefacts and pottery, clearly demonstrate that the aeolian dune excavated at Oudenaarde “Markt” was occupied by prehistoric men at different moments. The oldest activities obviously date back to pre-Holocene times. The lithic artefacts collected within the dune sediments present clear typological and technological affinities with Final Palaeolithic industries. Unfortunately, the assemblage is too small to allow for a further chronological precision. However, more chronological guidance is offered by the OSL-dates. Despite some inconsistencies in the lowest levels, the OSL-date for sample GLL-163916 (11.3 TAW), which stratigraphically corresponds to the level with the highest number of (large) artefacts, dates to the Younger Dryas and/or Preboreal. The Preboreal, however, can be excluded based on the presence of a silty cap on most larger artefacts, indicating that the latter were exposed to periglacial conditions. Whether the artefacts from the lower levels corresponding to the base of the dune date to the same age is difficult to assess. OSL sample GLL-163910 suggests a date between ca. 18,300 and 15,300 a. However, since no sites or artefacts are known in the entire Scheldt basin from this time-period, which corresponds to the final Pleniglacial, it seems highly unlikely that this date can be applied to the lithic industry.

It thus seems that the Younger Dryas is the most likely age estimate for the lithic assemblage from the dune sediments, although a date earlier in the Lateglacial (e. g. Older Dryas/Allerød) remains possible given the limit on the time-resolution that can be achieved using OSL dating (typically 6-10 %, 1 sigma). This is particularly interesting given the scarcity of sites dated to the Allerød (*Federmesser* Culture) and Younger Dryas (epi-Ahrensburgian like complexes) in and along the floodplain of the Scheldt and its tributaries (Crombé, in press a; Crombé & Robinson, 2017). So far no *Federmesser* sites

and only 3 to 4 Younger Dryas sites are known in this region. The latter are situated either on a dry river bank (Ruien “Rosalinde”), a scroll-bar (Wichelen “Wijmeersen”) or a dune (Oudenaarde “Markt”). This might indicate that the Younger Dryas occupation focused on river valleys, in contrast with the preceding *Federmesser* Culture of the Allerød, which had a preference for inland freshwater lakes (Crombé, in press a). As suggested in a recent paper (Crombé, in press b), this shift in occupation focus from lakes to rivers might have been triggered by a sudden lowering of the groundwater table at the transition from the Final Allerød to the Younger Dryas, which led to an almost complete disappearance of the inland lakes and ponds (cf. Bos et al., in this volume).

The site of Oudenaarde furthermore demonstrates that the dunes along the Scheldt and its tributaries, which are still numerous (Bogemans et al., 2012), have a considerable potential for Final Palaeolithic research, in particular into the Younger Dryas. However, finding sites in these contexts implies that the standard augering methods ought to be refined (Crombé & Verhegge, 2015). To date, the survey for prehistoric sites within development-led archaeology is too often restricted to the top 0.5 m of the Pleistocene sediments (De Clercq et al., 2012). The site of Oudenaarde, just like Ruien and Wichelen, demonstrates that Younger Dryas sites are generally situated deeper and can thus only be discovered when auger sampling and sieving is done over the entire depth of the aeolian sediments. In addition, the lack of reference layers, such as podzol horizons or organic paleosols within these sediments, implies that sampling needs to be done in a continuous “blind” way.

With an age range of ca. 6,500-5,100 a. the uppermost OSL date falls perfectly within the chronological range of the middle and late Neolithic. Fragments of flint-tempered pottery and lithics, such as polished tools, triangular and transverse arrowheads and a pointed blade, typical of this stage have been collected from the upper sediments, testifying of renewed human activity on the dune. The latter might be responsible for a local reactivation of aeolian activity, which led to the (re)deposition of sands on top of the Younger Dryas sands. Human-triggered dune reactivation at the onset of the Neolithic is well attested within the European sand-belt (Tolksdorf & Kaiser, 2012). However, considering possible taphonomic processes it may well be that this uppermost OSL-date at Oudenaarde is incorrect.

7. Conclusions

The fortuitous discovery of an aeolian dune with prehistoric occupations at Oudenaarde once again demonstrates the potential of city centers for prehistoric research. Despite its fragmented preservation due to extensive sand extraction, the excavation of this dune yielded important information on the earliest occupation of the site. This information would have been missed without the awareness of the excavators. Unfortunately, excavations in city centers are generally too much focused on the investigation of features, while little or no attention is given to the undisturbed sediment in between or below these features. Despite the frequent discovery of prehistoric artefacts in these contexts, this only incidentally gives rise to a further exploration of these undisturbed contexts, hence unique chances are missed to obtain information on the pre-Medieval occupation of our cities.

In addition, the excavations at Oudenaarde demonstrate the potential of future research on dunes along the floodplains of the Scheldt River and its tributaries. Further geo-archaeological research will definitely change our view on the Lateglacial and Early Holocene occupation of the Scheldt basin, which until now is very poorly understood.

Bibliography

ADAMIEC G. & AITKEN M. J., 1998. Dose-rate conversion factors: update. *Ancient TL*, 16: 37-50.

AITKEN M. J., 1976. Thermoluminescent age evaluation and assessment of error limits: revised system. *Archaeometry*, 18: 233-238.

AITKEN M. J., 1985. *Thermoluminescence Dating*. Academia press, London: 360 p.

AITKEN M. J. & ALLDRED J. C., 1972. The assessment of error limits in thermoluminescent dating. *Archaeometry*, 14: 257-267.

BERG-HANSEN I. M., in press. Alt Duvenstedt LA121 revisited - Blade technology in Ahrensburg culture. In: Eriksen B. V., Rensink E. & Harris E. (ed.), *Proceedings of the Amersfoort, Schleswig and Burgos meetings of the UISPP commission for "The Final Palaeolithic of Northern Eurasia"*.

BODU P., 2000. Les faciès tardiglaciaires à grandes lames rectilignes et les ensembles à pointes de Malaurie dans le sud du Bassin Parisien : quelques réflexions à partir du gisement du Closeau (Hauts-de-Seine). In: Crotti P. (ed.), *MESO '97. Actes de la Table ronde "Épipaléolithique et Mésolithique"*, Lausanne, 21-23 novembre 1997, Cahiers d'Archéologie Romande, 81, Lausanne: 9-28.

BOGEMANS F. & VANDENBERGHE D., 2011. OSL dating of an inland dune along the lower River Scheldt near Aard (East Flanders, Belgium). *Netherlands Journal of Geosciences*, 90 (1): 23-29.

BOGEMANS F., MEYLEMANS E., JACOBS J., PERDAEN Y., STORME A., VERDURMEN I. & DEFORCE K., 2012. The evolution of the sedimentary environment in the lower River Scheldt valley (Belgium) during the last 13,000 a BP. *Geologica Belgica*, 15 (1-2): 105-112.

BOSTYN F., MONCHABLON C., PRAUD I. & VANMONTFORT B., 2011. Le Néolithique moyen II dans le sud-ouest du Bassin de l'Escaut : nouveaux éléments dans le groupe de Spiere. In: Bostyn F., Martial E. & Praud I. (dir.), *Le Néolithique du nord de la France dans son contexte européen. Habitat et économie aux 4^e et 3^e millénaires avant notre ère. Actes du 29^e colloque interrégional sur le Néolithique. Villeneuve d'Ascq, 2-3 octobre 2009, (= Revue Archéologique de Picardie, N° spécial, 28): 55-76.*

BØTTER-JENSEN L., ANDERSEN L. E., DULLER G. A. T. & MURRAY A. S., 2003. Developments in radiation, stimulation and observation facilities in luminescence measurements. *Radiation Measurements*, 37: 535-541.

CROMBÉ P., in press (a). The environmental setting for the Lateglacial recolonisation of the Scheldt Basin (north-west Belgium) by the Federmesser-Gruppen. In: Grimm S. B., Mevel L., Sobkowiak-Tabaka I., Weber M.-J. (ed.), *Conference Proceedings "From the Atlantic to beyond the Bug river. Finding and defining the Federmesser-Gruppen / Azilian"*. Mainz (RGZM-Tagungen).

CROMBÉ P., in press (b). The impact of environmental changes on the human occupation of the Scheldt basin during the Younger Dryas. In: *Préhistoire de l'Europe du Nord-Ouest : mobilités, climats et identités culturelles. Amiens, 30 mai - 4 juin 2016. Actes du XXVIII^e du Congrès Préhistorique de France, Amiens.*

CROMBÉ P. & ROBINSON E., 2017. Human resilience to Lateglacial climate and environmental change in the Scheldt basin (NW Belgium). *Quaternary International*, 428: 50-63.

CROMBÉ P. & VERHEGGE J., 2015. In search of sealed Palaeolithic and Mesolithic sites using core sampling: the impact of grid size, meshes and auger diameter on the discovery probability. *Journal of Archaeological Science*, 53: 445-458.

CROMBÉ P., SERGANT J., VERBRUGGE A., DE GRAEVE A., CHERRETTÉ B., MIKKELSEN J., CNUUDE V., DE KOCK T., HUISMAN H. D. J., VAN OSS B. J. H., VAN STRYDONCK M. & BOUDIN M., 2014. A sealed flint knapping site from the Younger Dryas in the Scheldt valley (Belgium): Bridging the gap in human occupation at the Pleistocene-Holocene transition in W Europe. *Journal of Archaeological Science*, 50: 420-439.

DE CLERCQ W., BATS M., BOURGEOIS J., CROMBÉ P., DE MULDER G., DE REU J., HERREMANS D., LALOO P., LOMBAERT L., PLETS G., SERGANT J. & STICHELBAUT B., 2012. Development-led archaeology in Flanders: An overview of practices and results in the period 1990-2010. In: Webley L., Vander Linden M., Haselgrove C. & Bradley R. (ed.), *Development-led Archaeology in Northwest Europe. Proceedings of a Round-Table at the University of Leicester, 19th- 21st November 2009*, Oxbow Books, Oxbow: 29-55.

- DE CORTE F., VANDENBERGHE D., DE WISPELAERE A., BUYLAERT J.-P. & VAN DEN HAUTE P., 2006. Radon loss from encapsulated sediments in Ge gamma-ray spectrometry for the annual radiation dose determination in luminescence dating. *Czech Journal of Physics*, 56: D183-D194.
- DULLER G. A. T., 2003. Distinguishing quartz and feldspar in single grain luminescence measurements. *Radiation Measurements*, 37: 161-165.
- GOZDZIK J. S. & FRENCH H. M., 2004. Apparent Upfreezing of Stones in Late-Pleistocene Coversand, Belchato´w Vicinity, Central Poland. *Permafrost and Periglacial Processes*, 15: 359-366.
- JOHANSEN L. & STAPERT D., 2000. Two ‘Epi-Ahrensburgian’ sites in the northern Netherlands: Oudehaske (Friesland) and Gramsbergen (Overijssel). *Palaeohistoria*, 39/40: 1-87.
- JOHNSON D. L., MUHS D. R. & BARNHARDT M. L., 1977. The effects of frost heaving on objects in soils, II: Laboratory Experiments. *Plains Anthropologist*, 22 (76/1): 133-147.
- KAPLAR C. W., 1965. Stone migration by freezing of soil. *Science*, 149: 1520-1521.
- LAPP T., KOOK M., MURRAY A. S., THOMSEN K. J., BUYLAERT J.-P. & JAIN M., 2015. A new luminescence detection and stimulation head for the Risø TL / OSL reader. *Radiation Measurements*, 81: 178-184.
- LOMBAERT L., NOENS G. & AMEELS V., 2007. Een mesolithische vindplaats te Oudenaarde-Donk: een ruimtelijke, typologische en technische analyse. *Notae Praehistoricae*, 27: 89-99.
- MEJDAHL V., 1979. Thermoluminescence dating: beta-dose attenuation in quartz grains. *Archaeometry*, 21: 61-72.
- MURRAY A. S. & OLLEY J. M., 2002. Precision and accuracy in the optically stimulated luminescence dating of sedimentary quartz: a status review. *Geochronometria*, 21: 1-16.
- MURRAY A. S. & WINTLE A. G., 2000. Luminescence dating of quartz using an improved single-aliquot regenerative-dose protocol. *Radiation Measurements*, 32: 57-73.
- MURRAY A. S. & WINTLE A. G., 2003. The single aliquot regenerative dose protocol: potential for improvements in reliability. *Radiation Measurements*, 37: 377-381.
- NAUDINOT N., 2013. La fin du Tardiglaciaire dans le Grand-Ouest de la France. *Bulletin de la Société Préhistorique Française*, 110/2: 233-255.
- PARENT J.-P., VAN DER PLAETSEN P. & VANMOERKERKE J., 1986-1987. Prehistorische jagers en veetelers aan de Donk te Oudenaarde. *Vobov-info*, 24/25.
- PRESCOTT J. R. & HUTTON J. T., 1994. Cosmic ray contributions to dose rates for luminescence and ESR dating: large depths and long-term time variations. *Radiation Measurements*, 23: 497-500.
- SERGANT J., VANDENDRIESSCHE H., NOENS G., CRUZ F., ALLEMEERSCH L., ALUWÉ K., JACOPS J. WUYTS F., WINDEY S., ROZEK J., DEPAEPE I., HERREMANS D., LALOO P. & CROMBÉ P., 2016. Opgraving van een mesolithische wetlandsite te Kerkhove ‘Stuw’ (Avelgem, West-Vlaanderen): eerste resultaten. *Notae Praehistoricae*, 36: 47-57.
- TOLKSDORF J. F. & KAISER K., 2012. Holocene aeolian dynamics in the European sand-belt as indicated by geochronological data. *Boreas*, 41: 408-421.
- VALENTIN B., 1995. *Les groupes humains et leurs traditions dans le bassin Parisien. Apports de la technologie lithique comparée*. Thèse de doctorat de l’Université de Paris I, Paris: 864 p.
- VANDENBERGHE D., 2004. *Investigation of the optically stimulated luminescence dating method for application to young geological sediments*. PhD-thesis Universiteit Gent, Gent: 298 p.
- VANDENBERGHE D., DE CORTE F., BUYLAERT J.-P., KUČERA J. & VAN DEN HAUTE P., 2008. On the internal radioactivity in quartz. *Radiation Measurements*, 43: 771-775.
- VANDENBERGHE D., KASSE C., HOSSAIN S. M., DE CORTE F., VAN DEN HAUTE P., FUCHS M. & MURRAY A. S., 2004. Exploring the method of optical dating and comparison of optical and ¹⁴C ages of Late Weichselian coversands in the southern Netherlands. *Journal of Quaternary Science*, 19: 73-86.
- VANDENBERGHE D., VANNESTE K., VERBEECK K., PAULISSEN E., BUYLAERT J.-P., DE CORTE F. & VAN DEN HAUTE P., 2009. Late Weichselian and Holocene earthquake

events along the Geleen fault in NE Belgium: OSL age constraints. *Quaternary International*, 199: 56-74.

VANDENDRIESSCHE H., PEDE R., KLINKENBORG S., VERBRUGGE A., MIKKELSEN J., SERGANT J., CHERRETTÉ B. & CROMBÉ P., 2015. Steentijdvondsten uit het zuiden van Oost-Vlaanderen: het neolithicum te Leeuwergem-Spelaan (gem. Zottegem) en Ruien-Rosalinde (gem. Kluisbergen, BE). *Notae Praehistoricae*, 35: 5-23.

VAN GIJN A., 1990. *The Wear and Tear of Flint: Principles of Functional Analysis Applied to Dutch Neolithic Assemblages*. University of Leiden, Institute of Prehistory, Leiden (= *Analecta Praehistorica Leidensia*, 22).

VAN GIJN A., 2014. Science and interpretation in microwear studies. *Journal of Archaeological Science*, 48: 166-169.

VANMONTFORT B., 2001. The Group of Spiere as a New Stylistic Entity in the Middle Neolithic Scheldt Basin. *Notae Praehistoricae*, 21: 139-43.

VAN VLIET-LANOË B., 1985. Frost Effects in Soils. In: Boardman J., ed., *Soils and Quaternary Landscape Evolution*, John Wiley & Sons Ltd, London: 117-158.

WALLINGA J., 2002. Optically stimulated luminescence dating of fluvial deposits: a review. *Boreas*, 31: 303-322.

Acknowledgments

Luminescence research at Ghent University is partially funded by the Research Foundation-Flanders (FWO-Vlaanderen). The technical assistance of Ann-Eline Debeer is gratefully acknowledged. Thanks also to Annelies Storme (UGent) for assessing the pollen samples.

Abstract

Salvage excavations in the city center of Oudenaarde revealed remains of an aeolian dune formed on top of final Pleniglacial braided river sediments. OSL dating demonstrates that this dune was formed during the Lateglacial, most likely mainly during the Younger Dryas, a date confirming the Final Palaeolithic age of the associated industry. During the Middle to Late Neolithic the dune was reoccupied by the first farmers of the Scheldt basin, possibly leading to a reactivation of aeolian activity.

Keywords: Oudenaarde, prov. of East Flanders (BE), Scheldt River, dune, OSL, final Pleniglacial, Lateglacial, Younger Dryas, Final Palaeolithic, Neolithic.

Samenvatting

Tijdens preventief archeologisch onderzoek in het centrum van Oudenaarde werden de restanten van een eolische duin aan het licht gebracht, die zich bovenop vlechtende rivierafzettingen uit het finaal-Pleniglaciaal heeft gevormd. OSL-dateringen tonen aan dat deze duinvorming plaatsvond tijdens het Laat-Glaciaal en wellicht grotendeels in de Jonge Dryas en bevestigen tevens de finaal-paleolithische ouderdom van de geassocieerde lithische industrie. Een nieuwe occupatie van de duin tijdens het Neolithicum leidde mogelijk tot een heractivering van de eolische activiteit.

Trefwoorden: Oudenaarde, provincie Oost-Vlaanderen (BE), Schelde, duin, OSL-dateringen, finaal Pleniglaciaal, Laat-Glaciaal, Jonge Dryas, Finaal-Paleolithicum, Neolithicum.

Philippe CROMBÉ
Dimitri TEETAERT
Éva HALBRUCKER
Hans VANDENDRIESSCHE
Ghent University
Department of Archaeology
Section Prehistory
Sint-Pietersnieuwstraat, 35
BE – 9000 Gent
philippe.crombe@ugent.be
dimitri.teetaert@ugent.be
eva.halbrucker@ugent.be
hans.vandendriessche@ugent.be

Dimitri VANDENBERGHE
Johan DE GRAVE
Ghent University, Department of Geology
Laboratory of Mineralogy and Petrology
(Luminescence Research Group)
Krijgslaan, 281 (S8)
BE – 9000 Gent
davdenbe@gmail.com
Johan.DeGrave@ugent.be

Arne DE GRAEVE
Wouter DE MAEYER
SOLVA
Zuid III, Industrielaan, 25B
BE – 9320 Erembodegem
arne.de.graev@so-lva.be
wouter.de.maeyer@so-lva.be

Frédéric CRUZ
Gate bvba
Dorpsstraat, 73
BE – 8450 Bredene
FredericCruz@hotmail.com